

---

## STRANGENESS ENHANCEMENT AT THE HADRONIC CHEMICAL FREEZE-OUT

V.V. SAGUN,<sup>1</sup> D.R. OLIINYCHENKO,<sup>1,2</sup> K.A. BUGAEV,<sup>1</sup> J. CLEYMANS,<sup>3</sup>  
A.I. IVANYTSKYI,<sup>1</sup> I.N. MISHUSTIN,<sup>4,5</sup> E.G. NIKONOV<sup>6</sup>

<sup>1</sup>**Bogolyubov Institute for Theoretical Physics, Nat. Acad. of Sci. of Ukraine**  
(14b, Metrolohichna Str., Kyiv 03680, Ukraine; e-mail: v\_sagun@ukr.net)

<sup>2</sup>**FIAS, Goethe-University,**  
(Ruth-Moufang Str. 1, 60438 Frankfurt upon Main, Germany)

<sup>3</sup>**Department of Physics, University of Cape Town**  
(Rondebosch 7701, South Africa; e-mail: jean.cleymans@uct.ac.za)

<sup>4</sup>**FIAS, Goethe-University,**  
(Ruth-Moufang Str. 1, 60438 Frankfurt upon Main, Germany; e-mail: mishustin@fiас.uni-frankfurt.de)

<sup>5</sup>**Kurchatov Institute, Russian Research Center**  
(Kurchatov Sqr., Moscow, 123182, Russia)

<sup>6</sup>**Laboratory for Information Technologies, JINR**  
(141980 Dubna, Russia; e-mail: e.nikonov@jinr.ru)

PACS 25.75.-q, 25.75.Nq

The chemical freeze-out of hadrons created in the high energy nuclear collisions is studied within the realistic version of the hadron resonance gas model. The chemical non-equilibrium of strange particles is accounted via the usual  $\gamma_s$  factor which gives us an opportunity to perform a high quality fit with  $\chi^2/dof \simeq 63.5/55 \simeq 1.15$  of the hadronic multiplicity ratios measured from the low AGS to the highest RHIC energies. In contrast to previous findings, at low energies we observe the strangeness enhancement instead of a suppression. In addition, the performed  $\gamma_s$  fit allows us to achieve the highest quality of the Strangeness Horn description with  $\chi^2/dof = 3.3/14$ . For the first time the top point of the Strangeness Horn is perfectly reproduced, which makes our theoretical horn as sharp as an experimental one. However, the  $\gamma_s$  fit approach does not sizably improve the description of the multi-strange baryons and antibaryons. Therefore, an apparent deviation of multi-strange baryons and antibaryons from chemical equilibrium requires further explanation.

### 1. Introduction

The hadron yields measured in heavy ion collisions are traditionally analyzed by the Hadron Resonance Gas Model (HRGM) [1–4]. Its main assumption is an ex-

istence of the thermal equilibrium in the system under consideration, which is strongly supported by an excellent coincidence of experimental and theoretical yields of the hadrons built up from  $u$  and  $d$  quarks. Using the temperature  $T$ , the baryonic chemical potential  $\mu_B$  and isospin third component chemical potential  $\mu_{I3}$  the HRGM allows one to describe the hadronic multiplicities at the moment of chemical freeze-out (FO), the moment at which all inelastic reactions cease to exist. However, the HRGM has some traditional problems to describe the strange hadrons. Thus, within the standard HRGM formulation with a single hard-core repulsion radius for all particles the energy dependences of  $K^+/\pi^+$  and  $\Lambda/\pi^-$  ratios were never satisfactorily reproduced [1–3]. However, the non-monotonic energy dependence of  $K^+/\pi^+$  ratio, known as the Strangeness Horn, is of special interest because it may serve as a signal of the onset of deconfinement. In order to account for a deviation from the chemical equilibrium of strange hadrons the factor  $\gamma_s$  was introduced [5]. It is used to describe the undersaturated (oversaturated) densities  $\gamma_s < 1$  ( $\gamma_s > 1$ ) of each strange charge. Formally, the strange fugacity,

associated with each (anti)strange charge, is simply multiplied by the  $\gamma_s$  factor. Although the  $\gamma_s$  factor plays an important role in the analysis of the data measured in the collisions of elementary particles [3] and in the nucleus-nucleus collisions [3, 6], the problem of its justification remains unsolved. Also the results on the  $\gamma_s$  values obtained within different thermal models are controversial. For instance, a strong suppression of the strange charge in nucleus-nucleus collisions was reported in Ref. [3], while the results of Ref. [6] are consistent with  $\gamma_s = 1$ . In order to resolve the latter problem, we apply the most successful version of the HRGM with multicomponent hard-core repulsion [4, 7–10] to describe 111 independent hadron yield ratios measured at 14 values of the center of mass collision energy  $\sqrt{s_{NN}}$  in the interval from 2.7 GeV to 200 GeV.

The work is organized as follows. In the next section we give the theoretical basis of the present model. In Section 3 we present the data descriptions and discuss them. Section 4 is devoted to our conclusions.

## 2. Haddon Resonance Gas Model

We employ a multicomponent HRGM, which currently provides the best description of the observed hadronic multiplicities. It is the model developed in [4, 7–10]. The hadron interaction is taken into account via the hard-core repulsion whose radii have different values for pions  $R_\pi$ , kaons  $R_K$ , other mesons  $R_m$  and baryons  $R_b$ . The best global fit of all hadronic multiplicities was found for  $R_b = 0.2$  fm,  $R_m = 0.4$  fm,  $R_\pi = 0.1$  fm,  $R_K = 0.38$  fm [4]. The main equations of this HRGM are listed below, but more details can be found in [4, 7–10].

Let us consider the Boltzmann gas of  $N$  hadron species in a volume  $V$  that has the temperature  $T$ , the baryonic chemical potential  $\mu_B$ , the strange chemical potential  $\mu_S$  and the chemical potential of the isospin third component  $\mu_{I3}$ . The system pressure  $p$  and the  $K$ -th charge density  $n_i^K$  ( $K \in \{B, S, I3\}$ ) of the  $i$ -th hadron sort are given by the expressions

$$\frac{p}{T} = \sum_{i=1}^N \xi_i, \quad n_i^K = \frac{Q_i^K \xi_i}{1 + \frac{\xi_i^T \mathcal{B} \xi_i}{\sum_{j=1}^N \xi_j}}, \quad \xi = \begin{pmatrix} \xi_1 \\ \xi_2 \\ \dots \\ \xi_N \end{pmatrix}, \quad (1)$$

where  $\mathcal{B}$  denotes a symmetric matrix of the second virial coefficients with the elements  $b_{ij} = \frac{2\pi}{3}(R_i + R_j)^3$  and

the variables  $\xi_i$  are the solutions of the following system

$$\xi_i = \phi_i(T) \exp \left[ \frac{\mu_i}{T} - \sum_{j=1}^N 2\xi_j b_{ij} + \xi^T \mathcal{B} \xi \left[ \sum_{j=1}^N \xi_j \right]^{-1} \right], \quad (2)$$

$$\phi_i(T) = \frac{g_i}{(2\pi)^3} \int \exp \left( -\frac{\sqrt{k^2 + m_i^2}}{T} \right) d^3k. \quad (3)$$

Here the full chemical potential of the  $i$ -th hadron sort  $\mu_i \equiv Q_i^B \mu_B + Q_i^S \mu_S + Q_i^{I3} \mu_{I3}$  is expressed in terms of the corresponding charges  $Q_i^K$  and their chemical potentials,  $\phi_i(T)$  denotes the thermal particle density of the  $i$ -th hadron sort of mass  $m_i$  and degeneracy  $g_i$ , and  $\xi^T$  denotes the row of variables  $\xi_i$ . For each collision energy the fitting parameters are temperature  $T$ , baryonic chemical potential  $\mu_B$  and the chemical potential of the third projection of isospin  $\mu_{I3}$ , whereas the strange chemical potential  $\mu_S$  is found from the condition of vanishing strangeness.

In order to account for the possible strangeness non-equilibration we introduce the  $\gamma_s$  factor in a conventional way [5] by replacing  $\phi_i$  in Eqs. (2) and (3) as

$$\phi_i(T) \rightarrow \phi_i(T) \gamma_s^{s_i}, \quad (4)$$

where  $s_i$  is a number of strange valence quarks plus number of strange valence anti-quarks.

Width correction is taken into account by averaging all expressions containing mass by Breit-Wigner distribution having a threshold. As a result, the modified thermal particle density of  $i$ -th hadron sort acquires the form

$$\int \exp \left( -\frac{\sqrt{k^2 + m_i^2}}{T} \right) d^3k \rightarrow \frac{\int_{M_0}^{\infty} \frac{dx}{(x-m_i)^2 + \Gamma_i^2/4} \int \exp \left( -\frac{\sqrt{k^2 + x^2}}{T} \right) d^3k}{\int_{M_0}^{\infty} \frac{dx}{(x-m_i)^2 + \Gamma_i^2/4}}. \quad (5)$$

Here  $m_i$  denotes the mean mass of hadron and  $M_0$  stands for the threshold in the dominant decay channel. The main advantages of this approximation are a simplicity of its realization and a clear way to account for the finite width of hadrons. The effect of the vanishing resonances width or the Gaussian resonance width parameterization on the chemical FO parameters is discussed in [11].

The effect of resonance decay  $Y \rightarrow X$  on the final hadronic multiplicity is taken into account as  $n^{fin}(X) = \sum_Y BR(Y \rightarrow X) n^{th}(Y)$ , where  $BR(X \rightarrow X) = 1$  for the sake of convenience. The masses, the widths and the strong decay branchings of all experimentally known hadrons were taken from the particle tables used by the thermodynamic code THERMUS [12].

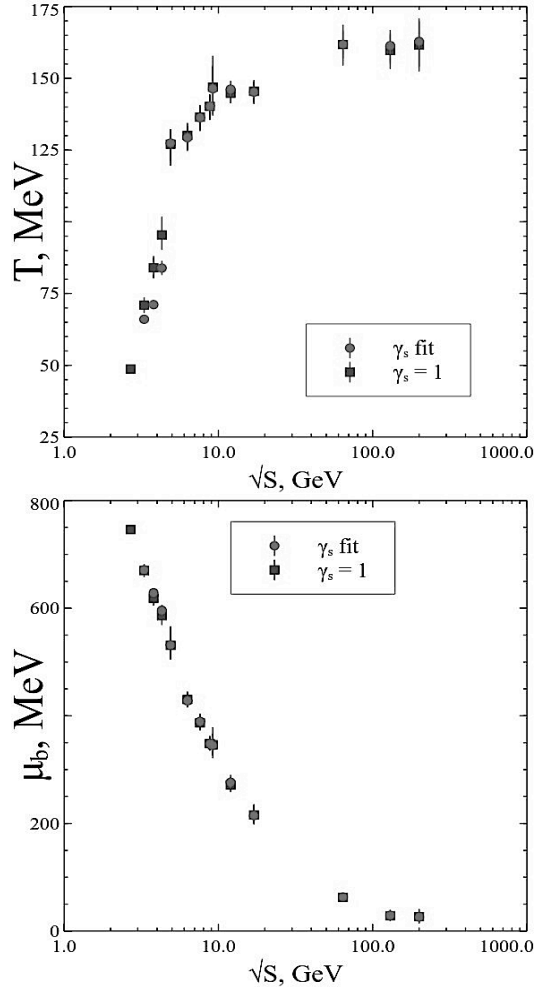


Fig. 1. Comparison of the parameters behavior for the  $\gamma_s$  fit and for the chemical FO model with  $\gamma_s = 1$ . Upper panel: the chemical FO temperature  $T$ . Lower panel: the chemical FO baryo-chemical potential  $\mu_B$ .

### 3. Results

**Data sets and fit procedure.** In this work we use the data set which is identical to Ref. [10]. At the AGS energies ( $\sqrt{s_{NN}} = 2.7 - 4.9$  AGeV or  $E_{lab} = 2 - 10.7$  AGeV) the data are available with a good energy resolution above 2 AGeV. However, for the beam energies 2, 4, 6 and 8 AGeV only a few data points are available. They correspond to the yields for pions [13, 14], for protons [15, 16], for kaons [14] (except for 2 AGeV). The integrated over  $4\pi$  data are also available for  $\Lambda$  hyperons [17] and for  $\Xi^-$  hyperons (for 6 AGeV only) [18]. However, as it was argued in Ref. [2], the data for  $\Lambda$  and  $\Xi^-$  should be recalculated for midrapidity. Therefore, instead of raw experimental data we used the corrected

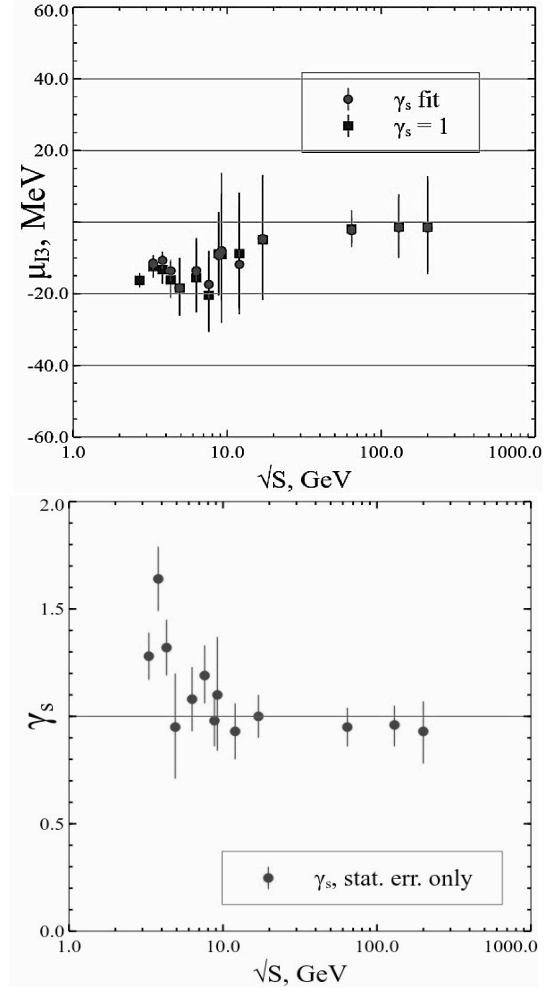


Fig. 2. Same as in Fig. (1), but for the chemical potential of the third projection of isospin  $\mu_{13}$  (upper panel) and the strangeness enhancement factor  $\gamma_s$  (lower panel) .

values from [2]. Further we analyzed the data set at the highest AGS energy ( $\sqrt{s_{NN}} = 4.9$  AGeV or  $E_{lab} = 10.7$  AGeV). Similarly to [4], here we analyzed only the NA49 mid-rapidity data [19–24] as the most difficult ones to be reproduced. Since the RHIC high energy data of different collaborations agree well with each other, we analyzed the STAR results for  $\sqrt{s_{NN}} = 9.2$  GeV [25],  $\sqrt{s_{NN}} = 62.4$  GeV [26],  $\sqrt{s_{NN}} = 130$  GeV [27–30] and 200 GeV [30–32].

The fit criterion is a minimization of  $\chi^2 = \sum_i \frac{(r_i^{ther} - r_i^{exp})^2}{\sigma_i^2}$ , where  $r_i^{ther}$  and  $r_i^{exp}$  are, respectively, theoretical and experimental values of particle yield ratios,  $\sigma_i$  stands for the corresponding experimental error and a summation is performed over all available experimental points.

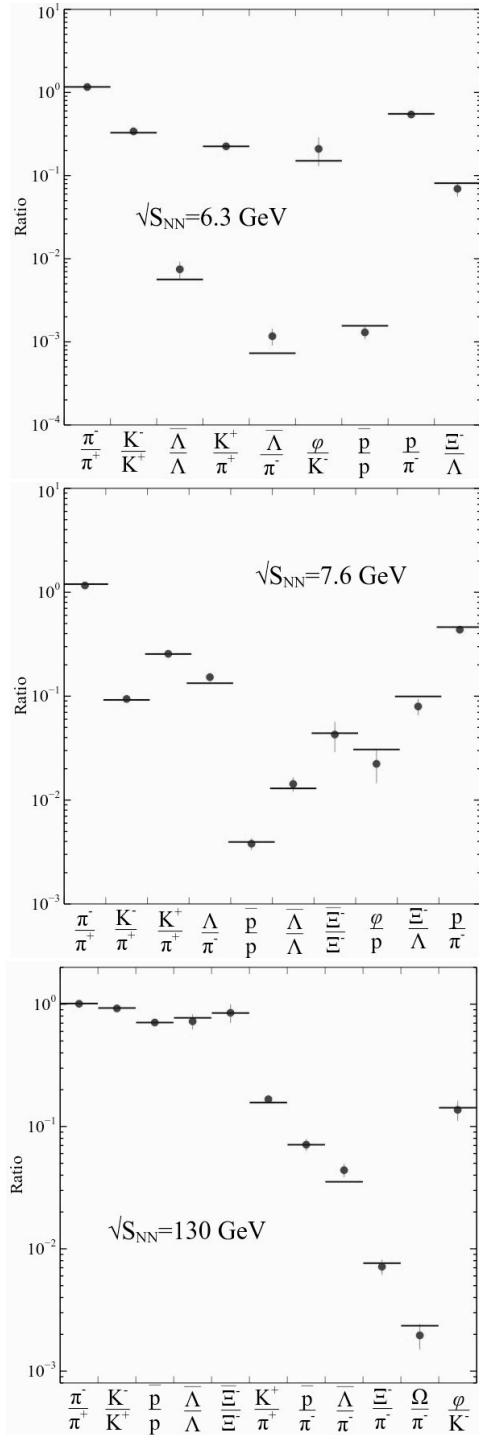


Fig. 3. The examples of the particle yield ratios description obtained for the  $\gamma_s$  fit. The dots denotes the experimental values, while the lines show the result of fit. The symbols on OX axis demonstrate the particle ratios. Upper panel:  $\sqrt{s_{NN}} = 6.3$  GeV,  $T = 129$  MeV,  $\mu_b = 427$  MeV. Middle panel:  $\sqrt{s_{NN}} = 7.6$  GeV,  $T = 136$  MeV,  $\mu_b = 389$  MeV. Lower panel:  $\sqrt{s_{NN}} = 130$  GeV,  $T = 161$  MeV,  $\mu_b = 29$  MeV.

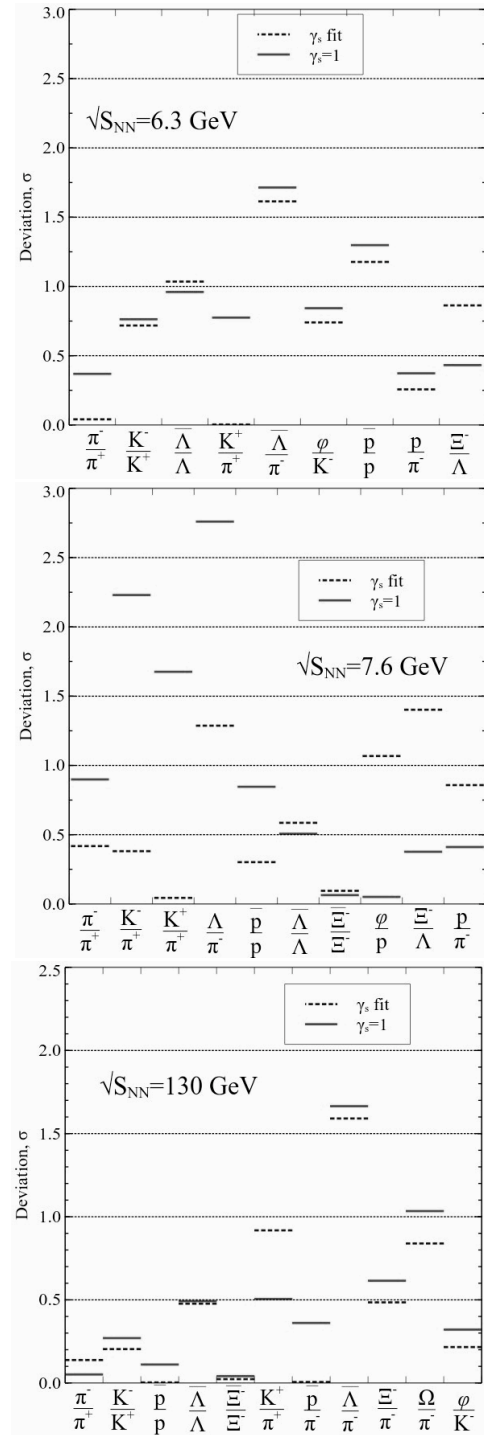


Fig. 4. Relative deviation of theoretical description of ratios from experimental value in units of experimental error  $\sigma$ . The symbols on OX axis demonstrate the particle ratios. OY axis shows  $\frac{|r^{theor} - r^{exp}|}{\sigma^{exp}}$ , i.e. the modulus of relative deviation for  $\sqrt{s_{NN}} = 6.3, 7.6$  and  $130$  GeV. Solid lines correspond to the model of chemical FO with  $\gamma_s = 1$ , while the dashed lines correspond to the model with the  $\gamma_s$  fit.

**The  $\gamma_s$  fit.** To improve the description of the strange hadrons and to investigate the role of their chemical non-equilibrium within the multicomponent HRGM we consider the  $\gamma_s$  factor as a fitting parameter for each value of collision energy. In our analysis we pay a special attention to the  $K^+/\pi^+$  ratio, because it is usually considered as the most problematic one for the HRGM.

For 14 collision energies  $\sqrt{s_{NN}} = 2.7, 3.3, 3.8, 4.3, 4.9, 6.3, 7.6, 8.8, 9.2, 12, 17, 62.4, 130, 200$  GeV the resulting fit quality  $\chi^2/dof = 63.4/55 = 1.15$  became slightly better compared to the result  $\chi^2/dof = 80.5/69 = 1.16$  found for the chemical FO model with  $\gamma_s = 1$ , although the value of  $\chi^2$  itself, not divided by number of degrees of freedom, has improved notably. As one can see from Figs. 1 and 2, the temperature, the baryo-chemical potential and the chemical potential of the isospin third projection obtained for the  $\gamma_s$  fit demonstrate almost the same behavior as for the case of the chemical FO model with  $\gamma_s = 1$ . The most remarkable behavior is demonstrated by the  $\gamma_s(\sqrt{s_{NN}})$  function (see the lower panel of 2). In contrast to the earlier results [3] we found not a strangeness suppression, but a sizable enhancement ( $\gamma_s > 1$ ) at the energies below  $\sqrt{s_{NN}} = 8.8$  GeV, while at higher energies our results  $\gamma_s \simeq 1$  are consistent with the findings of Ref. [6]. We have to stress, that our results on the  $\gamma_s$  fit have very high quality. This is clearly seen in Figs. 3, 4 and 5. At the same time the results of Ref. [3] have typical values of  $\chi^2/dof$  between 2 and 5 at each energy point, while our value  $\chi^2/dof = 63.4/55 = 1.15$  is given for all 111 independent ratios measured at 14 energies. Therefore, we conclude that the results on the strangeness suppression in heavy ion collisions reported in [3] are based on a low quality fit and, hence, they cannot be regarded as the statistically confident ones.

Now we study what ratios are improved at different energies. For AGS energies  $\sqrt{s_{NN}} = 2.7, 3.3, 3.8$  and 4.3 GeV the description quality is quite good even within the ideal gas model [2] since the number of model parameters equal or almost equal to the available number of ratios and only kaons and  $\Lambda$  contain strange quarks. Our detailed analysis demonstrate the fit instability for the low energies due to two local minima existence with very close  $\chi^2$  values. Thus, for  $\sqrt{s_{NN}} = 3.8$  GeV we obtained  $\gamma_s \simeq 1.6$  for the deepest minimum, while for another minimum, next to the deepest one,  $\gamma_s \simeq 0.8$ . An existence of two local minima with close values of  $\chi^2$  at  $\sqrt{s_{NN}} = 2.7 - 4.3$  GeV allows us to conclude that the  $\gamma_s$  concept has to be refined further in order to resolve this problem.

For the collision energy  $\sqrt{s_{NN}} = 4.9$  GeV there are no sizeable improvements compared to the  $\gamma_s = 1$  ap-

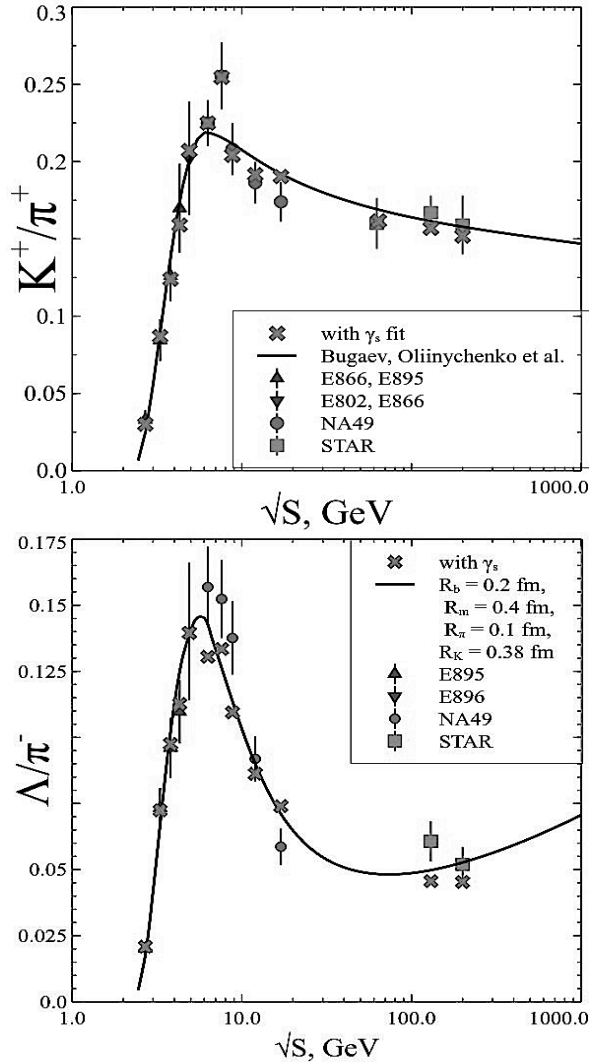


Fig. 5. Description of  $K^+/\pi^+$  ratio (upper plot) and  $\Lambda/\pi^-$  ratio (lower plot). Solid lines show the results of [4] for the HRGM with  $\gamma_s = 1$ . Crosses stand for the case of the  $\gamma_s$  fit.

proach [4]. The most significant data fit improvements are shown in Figs. 3, 4. At the energies  $\sqrt{s_{NN}} = 6.3 - 12$  GeV the  $K^+/\pi^+$  ratio is notably improved, while the description of other ratios was improved only slightly or even got worse. The typical examples of such a behavior are shown in the upper and middle panels of Fig. 4. At the same time for collision energy  $\sqrt{s_{NN}} = 130$  GeV we find the opposite data description behavior. The lower panel of Fig. 4 clearly demonstrates a fit quality improvement for all ten ratios except the  $K^+/\pi^+$  ratio.

An important result of the  $\gamma_s$  fitting approach is a precise Strangeness Horn description with  $\chi^2/dof = 3.3/14$ , i.e. even better than it was done in [4] with  $\chi^2/dof =$

7.5/14. Even the highest point of the Strangeness Horn is perfectly described now, that makes our theoretical Strangeness Horn as sharp as an experimental one (see upper panel on Fig. 5).

The obtained overall value  $\chi^2/dof \simeq 1.15$  for the  $\gamma_s$  fit is only slightly better compared to the result  $\chi^2/dof \simeq 1.16$  found in [4]. Moreover, the  $\gamma_s$  fit does not essentially improve either the ratios with the multistrange baryons or the  $\Lambda/\pi^-$  ratio (see the lower panel on Fig. 5) which is a consequence of the  $\bar{\Lambda}$  anomaly reported in [33, 34]. Therefore, we believe that further improvement of the data description is possible.

#### 4. Conclusions

We present an advanced description of the experimental hadron multiplicity ratios measured at AGS, SPS and RHIC energies. The inclusion of the  $\gamma_s$  factor into the recently developed version of the HRGM with the multicomponent hard-core repulsion has essentially improved the Strangeness Horn description to  $\chi^2/dof = 3.3/14$ , i.e. better than it was done recently in [4] with  $\chi^2/dof = 7.5/14$  and much better than it was done in [1–3, 6]. For the first time even the highest point of the Strangeness Horn is perfectly reproduced by our HRGM, which makes our theoretical horn as sharp as an experimental one. In contrast to earlier results reported in [3], we find that in heavy ion collisions there is a sizable enhancement of strangeness at low collision energies with  $\gamma_s \simeq 1.2 - 1.6$ . The achieved high quality fit of hadronic multiplicities with  $\chi^2/dof \simeq 63.5/55 \simeq 1.15$  gives us a high confidence in our conclusions. However, the present analysis shows that the  $\gamma_s$  fit does not sizably improve the description of the multi-strange baryons and antibaryons. Therefore, we conclude that the alternative approaches to the chemical FO suggested in [10, 35] should be developed further. We hope that the high quality data expected to be measured at the future heavy ion facilities will help us to understand the reason of the apparent chemical non-equilibrium of strange charge.

**Acknowledgments.** We would like to thank A. Andronic for providing an access to well-structured experimental data. K.A.B., D.R.O., A.I.I. and V.V.S. acknowledge a partial support of the Program ‘On Perspective Fundamental Research in High Energy and Nuclear Physics’ launched by the Section of Nuclear Physics of NAS of Ukraine. Also K.A.B. and I.N.M. acknowledge a partial support provided by the Helmholtz International Center for FAIR within the framework of the LOEWE program launched by the State of Hesse.

1. P. Braun-Munzinger, K. Redlich and J. Stachel, In \*Hwa, R.C. (ed.) et al.: Quark gluon plasma\*, **13**, 491 (2003).
2. A. Andronic, P. Braun-Munzinger and J. Stachel, Nucl. Phys. A **772**, 167 (2006) and references therein.
3. F. Becattini, J. Manninen and M. Gazdzicki, Phys. Rev. C **73**, 044905 (2006).
4. K.A. Bugaev, D.R. Oliinychenko, A.S. Sorin and G.M. Zinovjev, Eur. Phys. J. A **49**, 30–1-8 (2013) and references therein.
5. J. Rafelski, Phys. Lett. B **62**, 333 (1991).
6. P. Braun-Munzinger, D. Magestro, K. Redlich and J. Stachel, Phys. Lett. B **518**, 41 (2001).
7. G. Zeeb, K.A. Bugaev, P.T. Reuter and H. Stöcker, Ukr. J. Phys. **53**, 279 (2008).
8. D.R. Oliinychenko, K.A. Bugaev and A.S. Sorin, Ukr. J. Phys. **58**, 211 (2013).
9. K.A. Bugaev, D.R. Oliinychenko and A.S. Sorin, Ukr. J. Phys. **58**, 939 (2013).
10. K.A. Bugaev, D.R. Oliinychenko, J. Cleymans, A.I. Ivanytskyi, I.N. Mishustin, E.G. Nikonov, V.V. Sagun, Europhys. Lett. **104**, 22002 (2013).
11. K.A. Bugaev, A.I. Ivanytskyi, D.R. Oliinychenko, E.G. Nikonov, V.V. Sagun and G.M. Zinovjev, arXiv:1312.4367 [hep-ph].
12. S. Wheaton, J. Cleymans and M. Hauer, Comput. Phys. Commun. **180**, 84 (2009).
13. J.L. Klay *et al.*, Phys. Rev. C **68**, 054905 (2003).
14. L. Ahle *et al.*, Phys. Lett. B **476**, 1 (2000).
15. B.B. Back *et al.*, Phys. Rev. Lett. **86**, 1970 (2001).
16. J.L. Klay *et al.*, Phys. Rev. Lett. **88**, 102301 (2002).
17. C. Pinkenburg *et al.*, Nucl. Phys. A **698**, 495c (2002).
18. P. Chung *et al.*, Phys. Rev. Lett. **91**, 202301 (2003).
19. S.V. Afanasiev *et al.*, Phys. Rev. C **66**, 054902 (2002).
20. S.V. Afanasiev *et al.*, Phys. Rev. C **69**, 024902 (2004).
21. T. Anticic *et al.*, Phys. Rev. Lett. **93**, 022302 (2004).
22. S.V. Afanasiev *et al.*, Phys. Lett. B **538**, 275 (2002).
23. C. Alt *et al.*, Phys. Rev. Lett. **94**, 192301 (2005).
24. S.V. Afanasiev *et al.*, Phys. Lett. B **491**, 59 (2000).
25. B. Abelev *et al.*, Phys. Rev. C **81**, 024911 (2010).
26. B. Abelev *et al.*, Phys. Rev. C **79**, 034909 (2009).
27. J. Adams *et al.*, Phys. Rev. Lett. **92**, 182301 (2004).
28. J. Adams *et al.*, Phys. Lett. B **567**, 167 (2003).
29. C. Adler *et al.*, Phys. Rev. C **65**, 041901(R) (2002).
30. J. Adams *et al.*, Phys. Rev. Lett. **92**, 112301 (2004).
31. J. Adams *et al.*, Phys. Lett. B **612**, (2005) 181.
32. A. Billmeier *et al.*, J. Phys. G **30**, S363 (2004).
33. B.B. Back *et al.*, Phys. Rev. Lett. **87**, 242301 (2001).

34. J. Stachel, A. Andronic, P. Braun-Munzinger and K. Redlich, arXiv:1311.4662 [nucl-th].  
A.I. Ivanytskyi, J. Cleymans, E.G. Nikonov and G.M. Zinovjev, arXiv:1312.5149 [hep-ph].
35. K.A. Bugaev, D.R. Oliinychenko, V.V. Sagun,